Phys Chem Minerals (1997) 25:39–47

ORIGINAL PAPER

H. Yang · R.M. Hazen · L.W. Finger · C.T. Prewitt
R.T. Downs

Compressibility and crystal structure of sillimanite, Al_2SiO_5, at high pressure

Received December 16, 1996 / Revised, accepted February 26, 1997

Abstract The unit-cell dimensions and crystal structure of sillimanite at various pressures up to 5.29 GPa have been refined from single-crystal X-ray diffraction data. As pressure increases, *a* and *b* decrease linearly, whereas *c* decreases nonlinearly with a slightly positive curvature. The axial compression ratios at room pressure are $\beta_a:\beta_b:\beta_c$=1.22:1.63:1.00. Sillimanite exhibits the least compressibility along ***c***, but the least thermal expansivity along ***a*** (Skinner et al. 1961; Winter and Ghose 1979). The bulk modulus of sillimanite is 171(1) GPa with K'=4 (3), larger than that of andalusite (151 GPa), but smaller than that of kyanite (193 GPa). The bulk moduli of the [Al1O_6], [Al2O_4], and [SiO_4] polyhedra are 162(8), 269(33), and 367(89) GPa, respectively. Comparison of high-pressure data for Al_2SiO_5 polymorphs reveals that the [SiO_4] tetrahedra are the most rigid units in all these polymorphic structures, whereas the [AlO_6] octahedra are most compressible. Furthermore, [AlO_6] octahedral compressibilities decrease from kyanite to sillimanite, to andalusite, the same order as their bulk moduli, suggesting that [AlO_6] octahedra control the compression of the Al_2SiO_5 polymorphs. The compression of the [Al1O_6] octahedron in sillimanite is anisotropic with the longest Al1-OD bond shortening by ~1.9% between room pressure and 5.29 GPa and the shortest Al1-OB bond by only 0.3%. The compression anisotropy of sillimanite is primarily a consequence of its topological anisotropy, coupled with the compression anisotropy of the Al-O bonds within the [Al1O_6] octahedron.

Introduction

The Al_2SiO_5 polymorphs, sillimanite, andalusite, and kyanite, have been considered as primary thermobarometry for metamorphic rocks, because of their abundance in metamorphosed pelitic sediments and simple pressure-temperature phase equilibrium relations. From the crystal-chemical point of view, the Al_2SiO_5 polymorphs are of particular interest because Al occurs in three different coordinations; in addition to one-half of total Al that is octahedrally coordinated in each structure, the remaining Al is four-, five-, and six-coordinated in sillimanite, andalusite, and kyanite, respectively. Therefore, a detailed knowledge of the responses of three polymorphic structures, especially the different types of Al-O bonds, to high temperature and pressure is essential to the understanding of the crystal chemistry, physical properties, and phase relations of the Al_2SiO_5 polymorphs. The high-temperature crystal-chemistry of sillimanite, andalusite, and kyanite was investigated by Winter and Ghose (1979). Ralph et al. (1984) and Yang et al. (1997a) studied the pressure effects on the crystal structures of andalusite and kyanite, respectively. In this paper, we report a high-pressure X-ray structure study of sillimanite up to 5.29 GPa and compare our results with those for andalusite and kyanite to provide a better understanding of the high-pressure crystal-chemistry of the Al_2SiO_5 system.

The crystal structure of sillimanite was first determined by Taylor (1928) using X-ray diffraction intensities estimated from rotation photographs. Further structure refinements were carried out by Burnham (1963) and Winter and Ghose (1979) from single-crystal X-ray diffraction data. Neutron diffraction studies of the sillimanite structure were performed by Finger and Prince (1972) and Peterson and McMullan (1986). Summaries of crystal structural studies on three Al_2SiO_5 polymorphs have been given by Papike and Cameron (1976), Ribbe (1980), and Kerrick (1990).

H. Yang (✉) · R.M. Hazen · L.W. Finger · C.T. Prewitt
Geophysical Laboratory, 5251 Broad Branch Road, NW, Washington, DC 20015-1305

R.T. Downs
Department of Geosciences, University of Arizona, Tucson, Arizona 85721, USA

Experimental procedures

Room-pressure X-ray diffraction data measurements

The sample used in this study is from Reinbolt Hills, Antarctica, and was kindly supplied by Pete J. Dunn of the Smithsonian Insti-

Table 1 Crystal data and other relevant information on sillimanite at various pressures

P (GPa)	*a* (Å)	*b* (Å)	*c* (Å)	*V* (Å^3)	Total refls.	Refls. >3 σ (I)	R (int.)	Rw	R
0.00*	7.4857 (8)	7.6750 (9)	5.7751 (7)	331.80 (7)	532	409		0.036	0.033
0.65	7.4803 (13)	7.6600 (9)	5.7687 (11)	330.54 (6)					
1.23*	7.4732 (14)	7.6520 (9)	5.7631 (12)	329.56 (7)	1134	198	0.027	0.034	0.034
1.96	7.4595 (13)	7.6372 (9)	5.7580 (11)	328.03 (7)					
2.54*	7.4537 (11)	7.6238 (8)	5.7560 (10)	327.09 (6)	1112	195	0.030	0.027	0.029
3.22	7.4446 (12)	7.6094 (8)	5.7515 (11)	325.82 (7)					
3.72*	7.4345 (10)	7.5989 (7)	5.7507 (10)	324.88 (5)	1100	192	0.029	0.032	0.034
4.61	7.4224 (12)	7.5836 (8)	5.7462 (10)	323.44 (6)					
5.29*	7.4146 (12)	7.5739 (7)	5.7450 (10)	322.61 (6)	1086	185	0.028	0.029	0.030

* X-ray intensity data were collected at these pressures

Table 2 Atomic positional and isotropic displacement parameters of sillimanite at various pressures

P (GPa)		0.00	1.23	2.54	3.72	5.29
Al1	x	0	0	0	0	0
	y	0	0	0	0	0
	z	0	0	0	0	0
	B_{iso}	0.37 (2)	0.34 (3)	0.31 (3)	0.31 (3)	0.32 (3)
Al2	x	0.1417 (1)	0.1414 (2)	0.1411 (2)	0.1409 (2)	0.1405 (2)
	y	0.3452 (1)	0.3444 (2)	0.3437 (2)	0.3434 (2)	0.3427 (2)
	z	0.25	0.25	0.25	0.25	0.25
	B_{iso}	0.44 (2)	0.47 (4)	0.38 (4)	0.39 (4)	0.41 (4)
Si	x	0.1532 (1)	0.1536 (2)	0.1541 (2)	0.1543 (2)	0.1548 (2)
	y	0.3404 (1)	0.3394 (2)	0.3395 (2)	0.3389 (2)	0.3386 (2)
	z	0.75	0.75	0.75	0.75	0.75
	B_{iso}	0.42 (2)	0.43 (4)	0.44 (3)	0.43 (4)	0.47 (3)
OA	x	0.3602 (2)	0.3611 (5)	0.3618 (5)	0.3620 (5)	0.3633 (5)
	y	0.4089 (2)	0.4069 (5)	0.4062 (5)	0.4060 (5)	0.4055 (5)
	z	0.75	0.75	0.75	0.75	0.75
	B_{iso}	0.52 (3)	0.60 (8)	0.59 (8)	0.54 (8)	0.53 (8)
OB	x	0.3566 (2)	0.3554 (5)	0.3557 (4)	0.3559 (5)	0.3551 (5)
	y	0.4339 (2)	0.4348 (5)	0.4336 (5)	0.4334 (5)	0.4330 (5)
	z	0.25	0.25	0.25	0.25	0.25
	B_{iso}	0.55 (3)	0.48 (8)	0.39 (7)	0.51 (8)	0.60 (8)
OC	x	0.4767 (2)	0.4758 (5)	0.4748 (5)	0.4745 (5)	0.4728 (5)
	y	0.0009 (2)	0.0010 (7)	0.0021 (7)	0.0028 (7)	0.0031 (7)
	z	0.75	0.75	0.75	0.75	0.75
	B_{iso}	0.91 (4)	0.87 (8)	0.81 (7)	0.78 (8)	0.76 (8)
OD	x	0.1255 (2)	0.1255 (3)	0.1262 (3)	0.1266 (3)	0.1269 (3)
	y	0.2232 (2)	0.2228 (3)	0.2219 (3)	0.2211 (3)	0.2204 (3)
	z	0.5145 (2)	0.5150 (7)	0.5141 (7)	0.5152 (7)	0.5146 (7)
	B_{iso}	0.63 (3)	0.47 (5)	0.56 (4)	0.51 (5)	0.53 (5)

tution [specimen no: NMNH 139740; also sample no. 566 described by Grew (1980)]. Because of its good quality, this sample has been used for optical absorption studies (Grew and Rossman 1976), determination of elastic constants (Vaughan and Weidner 1978), infrared absorption studies (Kieffer 1979), and low-temperature heat-capacity measurements (Robie and Hemingway 1984; Hemingway et al. 1991). The chemical composition of the sample reported by Grew (1980) is SiO_2, 36.73; Al_2O_3, 61.98; Fe_2O_3, 1.10 (wt.%) or $(Al_{1.98}Fe_{0.2})SiO_5$. A single-crystal fragment (0.11×0.08×0.04 mm) showing sharp diffraction profiles was selected from a crushed sample for the study. A Picker four-circle diffractometer equipped with a Mo X-ray tube (β-filtered) was used for all X-ray measurements. Unit-cell parameters were determined by fitting the positions of 18 reflections with $20° < 2\theta < 35°$ following the procedure of King and Finger (1979), yielding *a*=7.4857(8), *b*=7.6750(9), and *c*=5.7751(7) Å (Table 1). These values are comparable to those reported by Grew (1980) for the same material from powder X-ray diffraction: *a*=7.4885(7), *b*=7.6756(3), and *c*=5.7734(5) Å.

X-ray diffraction intensity data from one octant of reciprocal space with $0° \leq 2\theta \leq 60°$ were collected using ω scans of 1° width in step increments of 0.025° and 3-s per step counting time. Two standard reflections were checked every 5 hours; no significant or systematic variations in intensities of the standard reflections were observed. Digitized step data were integrated by the method of Lehmann and Larsen (1974) with background manually reset when necessary. Corrections were made for Lorentz and polarization effects, but not for X-ray absorption by the crystal (μ=10.95 cm^{-1}).

The initial structural model of sillimanite was taken from Winter and Ghose (1979). Least-squares refinements were performed using an updated version of RFINE4 (Finger and Prince 1975) in the space group *Pbnm*. The small amount of Fe was ignored in the refinements and the structure was assumed to have an ideal composition of Al_2SiO_5 with the Al1 and Al2 sites fully occupied by Al and the Si site

Table 3 Selected interatomic distances (Å) in sillimanite at various pressures

P (GPa)	0.00	1.23	2.54	3.72	5.29
Al1-OA (x2)	1.915 (1)	1.913 (3)	1.909 (3)	1.905 (3)	1.898 (3)
Al1-OB (x2)	1.869 (1)	1.869 (2)	1.867 (2)	1.863 (2)	1.864 (2)
Al1-OD (x2)	1.956 (2)	1.948 (2)	1.937 (2)	1.928 (2)	1.918 (2)
Avg.	1.913	1.910	1.904	1.899	1.893
Al2-OB	1.747 (2)	1.742 (4)	1.740 (4)	1.739 (4)	1.732 (4)
Al2-OC	1.709 (2)	1.712 (5)	1.708 (5)	1.702 (5)	1.706 (5)
Al2-OD (x2)	1.796 (1)	1.792 (4)	1.785 (4)	1.789 (4)	1.783 (4)
Avg.	1.762	1.760	1.755	1.755	1.751
Si-OA	1.636 (2)	1.634 (4)	1.630 (4)	1.626 (4)	1.627 (4)
Si-OC	1.569 (2)	1.570 (5)	1.568 (5)	1.571 (5)	1.564 (5)
Si-OD (x2)	1.644 (1)	1.635 (4)	1.640 (4)	1.633 (4)	1.635 (4)
Avg.	1.623	1.619	1.620	1.616	1.615

Table 4 Selected interatomic angles (°) in sillimanite at various pressures

P (GPa)	0.00	1.23	2.54	3.72	5.29
OA-Al1-OB	99.8 (1)	99.6 (1)	99.7 (1)	99.8 (1)	99.9 (1)
OA-Al1-OB'	80.3 (1)	80.4 (1)	80.3 (1)	80.2 (1)	80.1 (1)
OA-Al1-OD	88.6 (1)	88.2 (2)	88.1 (2)	88.3 (2)	88.1 (2)
OA-Al1-OD'	91.4 (1)	91.8 (2)	91.9 (2)	91.7 (2)	91.9 (2)
OB-Al1-OD	90.3 (1)	90.6 (2)	90.6 (2)	90.5 (2)	90.7 (2)
OB-Al1-OD'	89.7 (1)	89.4 (2)	89.4 (2)	89.5 (2)	89.3 (2)
OB-Al2-OC	113.3 (1)	112.9 (2)	113.3 (2)	113.5 (2)	113.5 (2)
OB-Al2-OD	105.4 (1)	105.5 (1)	105.2 (1)	105.0 (1)	104.9 (1)
OC-Al2-OD	108.2 (1)	108.1 (1)	108.2 (1)	108.3 (1)	108.3 (1)
OD-Al2-OD'	116.6 (1)	116.9 (2)	116.8 (2)	116.9 (2)	117.0 (2)
OA-Si-OC	109.6 (1)	109.6 (2)	109.6 (2)	109.3 (2)	109.1 (2)
OA-Si-OD	107.2 (1)	107.1 (1)	106.9 (1)	106.9 (1)	106.9 (1)
OC-Si-OD	110.6 (1)	110.5 (1)	110.8 (1)	111.0 (1)	111.1 (1)
OD-Si-OD'	111.7 (1)	111.8 (2)	111.7 (2)	111.6 (2)	111.6 (2)
Al1-OA-Si	129.4 (1)	129.2 (1)	129.0 (1)	129.0 (1)	128.7 (1)
Al1-OB-Al2	129.4 (1)	129.6 (1)	129.5 (1)	129.5 (1)	129.6 (1)
Al2-OC-Si	172.0 (1)	171.7 (3)	171.3 (3)	170.0 (3)	170.4 (3)
Al1-OD-Al2	116.9 (1)	116.7 (2)	116.7 (2)	116.3 (2)	116.3 (2)
Al1-OD-Si	125.1 (1)	125.2 (2)	125.0 (2)	125.2 (2)	125.1 (2)
Al2-OD-Si	114.2 (1)	114.5 (1)	114.4 (1)	114.4 (1)	114.4 (1)
OB-OA-OB	172.3 (1)	171.4 (2)	171.5 (2)	171.5 (2)	171.4 (2)
$[SiO_4]$ OTPA	19.75 (3)	19.58 (6)	19.41 (6)	19.35 (6)	19.05 (6)
$[Al2O_4]$ OPTA	27.75 (3)	27.89 (6)	28.21 (6)	28.32 (6)	28.62 (6)

* OPTA – out of-plane tilting angle (see the text for definition)

by Si. Neutral atomic scattering factors, including anomalous dispersion corrections for Al, Si, and O, were taken from Ibers and Hamilton (1974). Weighting schemes were based on $w=[\sigma^2(F)+(pF)^2]^{-1}$, where p is adjusted to ensure that the errors were normally distributed through probability plot analysis (Ibers and Hamilton 1974). Type II isotropic extinction corrections (Becker and Coppens 1975) were applied in the refinements. Atomic positional coordinates and isotropic displacement parameters are presented in Table 2.

High-pressure X-ray diffraction data measurements

After the X-ray intensity data collection at room pressure, the crystal was mounted in a Merrill-Bassett diamond-anvil cell with a mixture of 4:1 methanol:ethanol as the pressure medium. Four small (~10 μm) ruby chips were included as the internal pressure calibrant (Mao et al. 1986), from which pressure was determined from the position of the R_1 laser-induced fluorescence peak, with an error of approximately 0.05 GPa. The fixed-ϕ mode of data measurement (Finger and King 1978) was employed throughout the high-pressure experiments to maximize reflection accessibility and minimize attenuation by the diamond cell. Lattice constants were determined using the same method as described for the room-pressure experiment.

X-ray diffraction intensities were collected at 1.23, 2.54, 3.72, and 5.29 GPa for all accessible reflections with $0°\leq 2\theta \leq 60°$. The experimental procedures for X-ray data collection, reduction, and structure refinements were similar to those described above for the data collected at room pressure. In addition, corrections were made for absorption by the diamond and beryllium components of the pressure cell. After the data collection at 5.29 GPa, the pressure of the crystal was raised to 5.62 GPa. However, some peak profiles of reflections used to determine the unit-cell dimensions became significantly broadened at this pressure; thus, no further attempt was made to collect X-ray diffraction data at or above this pressure. Unit-cell dimensions and final refinement statistics are given in Ta-

Table 5 Polyhedral volumes ($Å^3$) and distortion indices of sillimanite at various pressures

P (GPa)		0.00	1.23	2.54	3.72	5.29
$[Al1O_6]$	V*	9.197 (8)	9.150 (16)	9.066 (15)	8.985 (16)	8.907 (16)
	QE	1.0107 (1)	1.0105 (2)	1.0105 (2)	1.0106 (2)	1.0108 (2)
	AV	35.4 (1)	35.1 (3)	35.8 (3)	36.3 (3)	37.4 (3)
$[Al2O_4]$	V	2.782 (3)	2.772 (9)	2.747 (9)	2.745 (9)	2.728 (9)
	QE	1.0062 (1)	1.0061 (2)	1.0064 (2)	1.0070 (2)	1.0070 (2)
	AV	20.4 (2)	20.4 (4)	21.6 (4)	22.29 (4)	23.5 (4)
$[SiO_4]$	V	2.192 (3)	2.174 (8)	2.177 (8)	2.161 (8)	2.159 (8)
	QE	1.0014 (1)	1.0015 (1)	1.0015 (1)	1.0014 (1)	1.0016 (1)
	AV	3.6 (1)	3.8 (2)	4.3 (2)	4.3 (2)	4.6 (2)

* V – polyhedral volume; QE – quadratic elongation; AV – angle variance (Robinson et al. 1971)

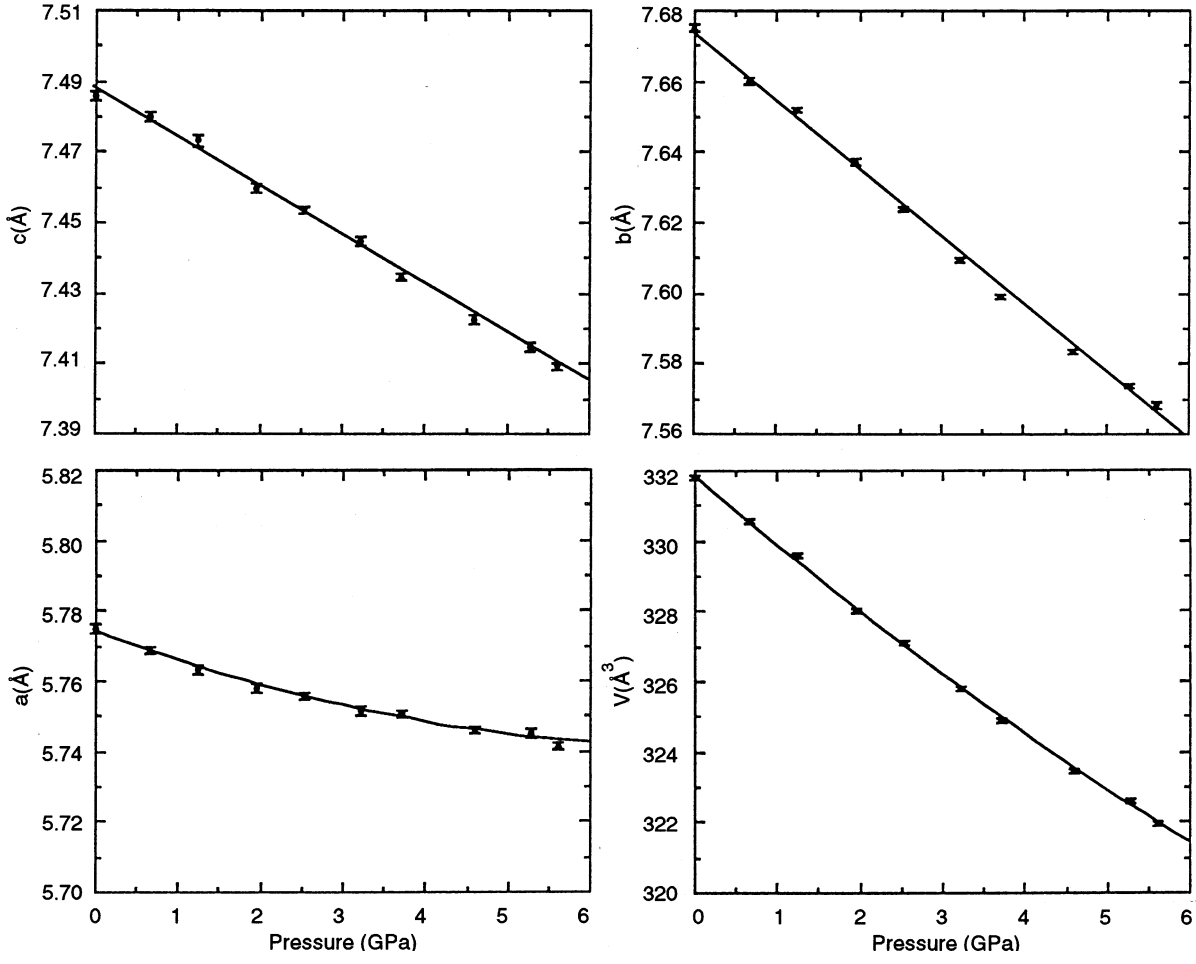

Fig. 1 Unit-cell parameters of sillimanite as a function of pressure

ble 1; atomic positional and isotropic displacement parameters are listed in Table 2; selected interatomic distances and angles are presented in Table 3 and 4, respectively. Polyhedral volumes and distortion indices are given in Table 5.

Results

Unit-cell compressibilities and bulk modulus

Figure 1 plots the unit-cell parameters of sillimanite as a function of pressure. With increasing pressure, *a* and *b* decrease linearly, whereas *c* decreases nonlinearly with a positive curvature, reflecting the increase in the stiffening of the structure along ***c*** at higher pressures. As a consequence, the unit-cell volume also decreases nonlinearly with a slightly positive curvature as pressure increases. The linear compressibilities of the *a* and *b* cell dimensions (β_a and β_b) are 0.00187(4) and 0.00250(5) GPa^{-1}, respectively, whereas β_c is 0.00153 (4) GPa^{-1} at room pressure and 0.00046(5) GPa^{-1} at 5.29 GPa. Thus, there is a considerable increase in the unit-cell compressional anisotropy with increasing pressure. The axial compression ratios (β_a: β_b: β_c) change from 1.22:1.63:1.00 at room pressure to 4.07:5.43:1 at 5.29 GPa. Weighted volume and pres-

sure data fit to a second-order Birch-Murnaghan equation of state yields V_0=331.81(5) Å^3, K_0 =171(7) GPa, and K'=4(3).

Structural variations with pressure

Three different polyhedra form the sillimanite structure: the [Al1O_6] octahedron, and the [Al2O_4] and [SiO_4] tetrahedra. All Al-O bond lengths within the [Al1O_6] octahedron decrease nearly linearly with increasing pressure (Fig. 2). The linear compressibilities of individual Al1-O bond distances appear to be a function of their length. Between room pressure and 5.29 GPa, the shortest Al1-OB bond compresses by ~0.3%, whereas the longest Al1-OD bond compresses by ~1.9%. The average Al1-O bond distance shortens by ~1.0% over this pressure range with a linear compressibility of 0.00204 GPa^{-1}. Correspondingly, the [Al1O_6] octahedral volume changes from 9.197(8) to 8.907(16) Å^3; the octahedral bulk modulus is 162(8) GPa.

At room pressure, the Al atom within the [Al2O_4] tetrahedron and the Si atom within the [SiO_4] tetrahedron are displaced substantially toward the bridging OC atom such that the Al2-OC and Si-OC bond distances (1.709 and 1.569 Å, respectively) are abnormally short, as noted by Burnham (1963). Within the experimental errors, these two short bond distances are virtually unaffected by pressure up to 5.29 GPa. Compared to the average Si-O bond distance, the relatively longer average Al2-O bond length is more compressible; between room pressure and 5.29 GPa, the average Al2-O bond distance decreases by 0.6% (β=0.00118 GPa^{-1}), whereas the average Si-O bond length shortens by 0.5% (β=0.00089 GPa^{-1}). Similarly, the volume of the [Al2O_4] tetrahedron shows a larger decrease (1.9%) in the experimental pressure range than that of the [SiO_4] tetrahedron (1.5%). The bulk moduli of the [Al2O_4] and [SiO_4] tetrahedra are 269(33) and 367(89) GPa, respectively.

Due to the sharing of OA-OB edges, the [Al1O_6] octahedron in sillimanite at room pressure is considerably distorted, as measured by the polyhedral quadratic elongation (QE) and angle variance (AV) (Robinson et al. 1971). Within the experimental uncertainties, the [Al1O_6] octahedral quadratic elongation does not change significantly as a function of pressure, whereas its angle variance increases slightly from 35.4(1) at room pressure to 37.4(3) at 5.29 GPa. The QE values of the [Al2O_4] and [SiO_4] tetrahedra are also essentially unchanged between room pressure and 5.29 GPa, while their AV values increase from 20.4(2) and 3.6(1) to 23.5(4) and 4.6(2), respectively.

The pressure effects on the relative orientations of the [Al1O_6], [Al2O_4], and [SiO_4] polyhedra are also apparent. For instance, between room pressure and 5.29 GPa, the Al1-OA-Si and Al2-OC-Si angles decrease from 129.4(1) and 172.0(1)° to 128.7(1) and 170.4(3)°, respectively. The angle between ***b*** and the Al1-OD bond, the most compressible bond within the [Al1O_6] octahedron,

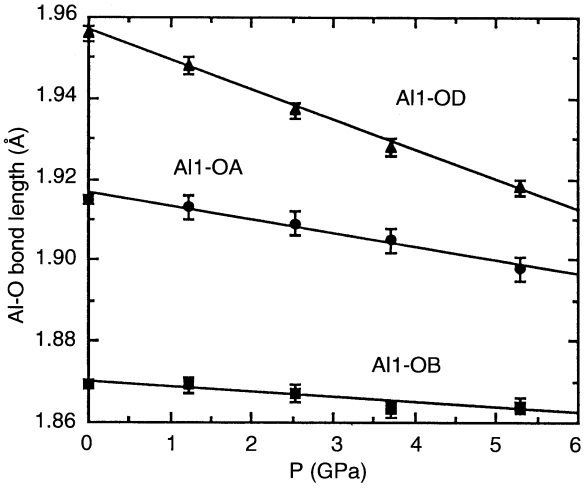

Fig. 2 Variations of the Al-O bond distances within the [AlO_6] octahedron with pressure

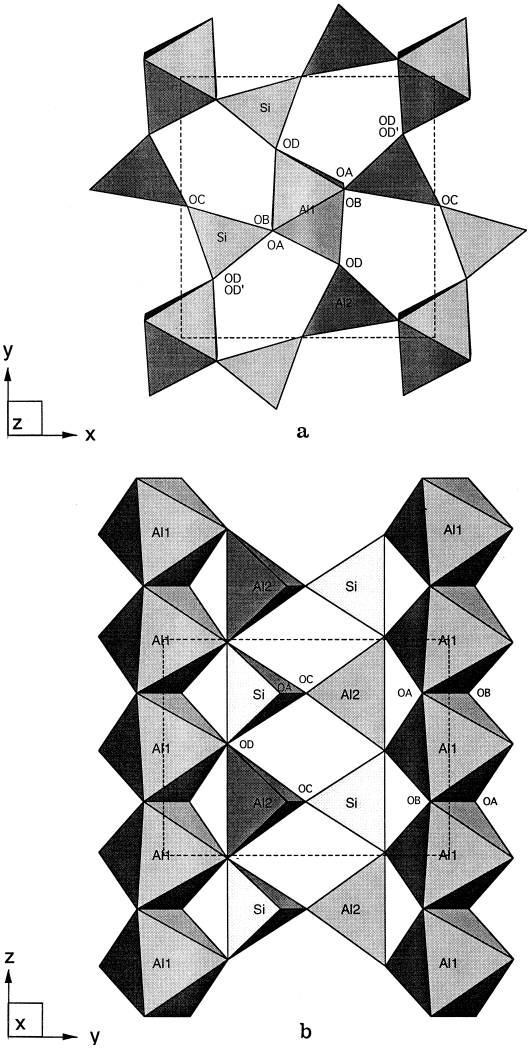

Fig. 3 a Crystal structure of sillimanite projected down c and **b** down a

changes from 28.84(3)° at room pressure to 29.51(7)° at 5.29 GPa. Because the interatomic bond angles within the [Al1O_6] octahedron do not change significantly with pressure (Table 4), the increase in the angle between ***b*** and the Al1-OD bond indicates a relatively clockwise rotation for the [Al1O_6] octahedra located at the unit-cell corners as pressure increases and an anti-clockwise rotation for the octahedra at the center of the unit cell (Fig. 3a). The change in the relative orientations of the [Al2O_4] and [SiO_4] tetrahedra can also be described by the out-of-plane tilting angle, the angle between the (100) plane and one of the tetrahedral faces defined by the OC, OD, and OD' atoms (Fig. 3a). This angle decreases from 19.75(3)° at room pressure to 19.05(6)° at 5.29 GPa for the [SiO_4] tetrahedron, but increases from 27.75(3)° to 28.62(6)° for the [Al2O_4] tetrahedron (Table 4).

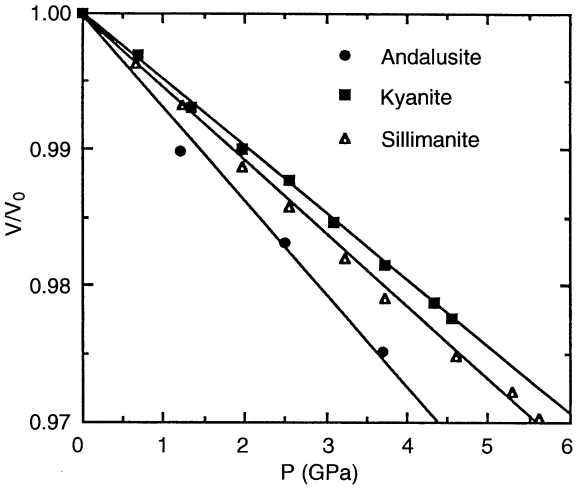

Fig. 4 Relative compressibilites (V/V0) of andalusite (Ralph et al. 1984), kyanite (Yang et al. 1996a), and sillimanite as a function of pressure

Discussion

Bulk moduli of the Al_2SiO_5 polymorphs

The isothermal compressibilities of the Al_2SiO_5 polymorphs were first determined by Brace et al. (1969); the bulk moduli calculated from their data are 127(3), 133(2), 132(5) GPa for kyanite, andalusite, and sillimanite, respectively. Using the Brillouin scattering technique, Vaughan and Weidner (1978) obtained the respective bulk moduli of 166 and 175 GPa (Voigt bound values) or 158 and 166 GPa (Reuss bound values) for andalusite and sillimanite. The bulk moduli determined from high-pressure single-crystal X-ray diffraction data are 135(10) GPa for andalusite (Ralph et al. 1984), 193(1) GPa for kyanite (Yang et al. 1996a), and 171(1) GPa for sillimanite (This study). Our value for sillimanite is in agreement with that of Vaughan and Weidner (1978). It also agrees well with the value of 175 GPa derived by Matsui (1996) for sillimanite based on the molecular dynamics calculation. However, there is a significant difference between the bulk moduli for andalusite reported by Vaughan and Weidner (1978) and Ralph et al. (1984). According to Ralph et al. (1984), this discrepancy is unlikely to originate from the difference between isothermal and adiabatic bulk moduli because the correction for the two different moduli is only on the order of 0.1%. An examination of the unit-cell parameters reported by Ralph et al. (1984) suggests that the smaller bulk modulus of andalusite obtained by Ralph et al. (1984) could stem from the unit-cell volume data they used in the calculation. In their study on andalusite, Ralph et al. (1984) did not directly measure the room-pressure unit-cell parameters of the crystal they used for the high-pressure study; instead, they adopted the room-pressure data from Winter and Ghose (1979). These two groups of workers used different methods for their unit-cell dimension measurements. By summarizing all available unit-cell parameters for andalusite from Minas Gerais, Brazil [the same sample studied by Winter and Ghose (1979) and Ralph et al. (1984)], Robie and Hemingway (1984) noticed that the room-pressure unit-cell volume of 342.45(6) Å^3 given by Winter and Ghose (1979) is significantly larger than are the other values (~342.00 Å^3) (e.g., Skinner et al. 1961; Burnhan and Buerger 1961; Brace et al. 1969; Holdaway 1971). To be consistent with the high-pressure data determined by Ralph et al. (1984), we re-determined the unit-cell parameters of the andalusite crystal from Minas Gerais, Brazil (NMNH R3717) using the same method as that employed by Ralph et al. (1984). The unit-cell dimensions we obtained are a=7.7939(5), b=7.8978(6), c=5.5544(4) Å, and V= 341.90(4) Å^3. Refitting the high-pressure data of Ralph et al. (1984) with the room-pressure unit-cell volume we determined in this study results in a bulk modulus of 151 (3) GPa for andalusite, which is comparable with the value given by Vaughan and Weidner (1978). Regardless of the possible difference between isothermal and adiabatic bulk moduli, it is evident that the bulk moduli for the Al_2SiO_5 polymorphs determined by the Brillouin scattering technique and high-pressure single-crystal X-ray diffraction decrease as the polymorphic molar volumes increase from kyanite, sillimanite, to andalusite. Figure 4, which plots V/V_0 as a function of pressure, illustrates the relative compressibilities of the three Al_2SiO_5 polymorphs. The greater incompressibility of kyanite is attributed to the nearly cubic close-packed arrangement of oxygen atoms and the complex edge-sharing among four distinct [AlO_6] octahedra in its crystal structure (Yang et al. 1997a).

Polyhedral compressibilities

At high pressure, the [SiO_4] tetrahedra in three Al_2SiO_5 polymorphs are the most incompressible units of all various polyhedra; their bulk moduli are 410(150) GPa in andalusite (Ralph et al. 1984), 361(88) GPa in kyanite

(Yang et al. 1997a), and 367(89) GPa in sillimanite. On the other hand, the [AlO_6] octahedra are the most compressible units in all Al_2SiO_5 polymorphic structures. Moreover, the bulk moduli of the [AlO_6] octahedra appear to decrease in these structures as their octahedral volumes increase, with the largest octahedral bulk moduli found in kyanite (~247 GPa) (Yang et al. 1997a) and the smallest in andalusite (132 GPa) (Ralph et al. 1984), reinforcing the conclusion of Yang et al. (1997a). Note that the bulk modulus of kyanite is also the largest in three polymorphs and that of andalusite the smallest. This correlation suggests that the high-pressure behavior of [AlO_6] octahedra plays an important role in controlling the compressibilities of the Al_2SiO_5 polymorphs. A similar conclusion was drawn by Vaughan and Weidner (1978) based on their Brillouin scattering experiments on andalusite and sillimanite.

Angel (1988) and Downs et al. (1994) determined the structures of anorthite up to 3.1 GPa and low-albite up to 3.78 GPa, respectively. In contrast to our observations, they found little pressure dependence of the [AlO_4] tetrahedral volumes or the Al-O bond distances within the [AlO_4] tetrahedra. The rigid behavior of the [AlO_4] tetrahedra in anorthite and low-albite is understandable considering the relatively low pressure range and the great flexibility of the framework structures. However, owing to the symmetry restriction and the configurations of two types of polyhedral chains (Fig. 3), the structure flexibility of sillimanite is much less than that of anorthite or low-albite, especially along ***c***. Hence, when subjected to pressure, the Al-O bonds within the [$Al2O_4$] tetrahedron are no longer as rigid as those in anorthite and low-albite. In fact, the [$Al2O_4$] tetrahedron [bulk modulus= 267(23) GPa] in sillimanite is nearly as compressible as the [AlO_6] octahedra [average bulk modulus= 247(27) GPa] in kyanite (Yang et al. 1997a).

Compressional anisotropy

The compression anisotropy of sillimanite (β_a:β_b:β_c= 1.22:1.63:1.00) at room pressure is not as pronounced as that of andalusite (β_a:β_b:β_c=2.13:1.47:1.00) (Ralph et al. 1984), but it is more apparent than that of kyanite ($|\varepsilon_1|:|\varepsilon_2|:|\varepsilon_3|$=1.00:1.16:1.33) (Yang et al. 1997a). Note that kyanite is triclinic, so the unit strain coefficients of the compression ellipsoid are used for comparison. The compression anisotropy of sillimanite is primarily a result of its inherent structural anisotropy and the markedly differential compression of the Al-O bonds within the [$Al1O_6$] octahedron. As illustrated in Fig. 3, parallel to ***c*** are not only the edge-shared [$Al1O_6$] octahedral chains (a common structural feature shared by all three Al_2SiO_5 polymorphs), but also the corner-shared double [$Al2O_4$] and [SiO_4] tetrahedral chains. Octahedral chains are cross-linked by the relatively rigid tetrahedra through corner sharing, leaving open structural tunnels running parallel to ***c*** as well. Thus, the compression along ***a*** or ***b*** can be readily achieved through changes in the interpolyhedral angles or relative orientations of polyhedra, such as the out-of-plane tilting of the [$Al2O_4$] and [SiO_4] tetrahedra and the relative rotation of the [$Al1O_6$] octahedra in the *a*-*b* plane. Such a compression mechanism is rather common in the case of open structures, especially when these structures consist of relatively rigid polyhedral units (Hazen and Finger 1979, 1985; Comodi et al. 1990, 1991). In contrast, compression along ***c*** requires the compression of the polyhedra forming the two kinds of chains, which is normally more difficult than changes in interpolyhedral angles. Consequently, the sillimanite structure is least compressible along ***c***. The greater compressibility along ***b*** than that along ***a*** arises principally from the noticeably differential compression of the individual Al-O bonds within the [$Al1O_6$] octahedron. Of all cation-anion bonds in the structure, the longest Al1-OD bond, which lies nearly on the a-b plane at ~30° to ***b***, compresses most; it is twice as compressible as the Al1-OA bond and six times more so than the Al1-OB bond. Similar results have also been observed in andalusite (Ralph et al. 1984), in which the *a* dimension is more compressible than *b*, mainly because of the long Al1-OD bond lying on the *a*-*b* plane at ~30° to the *a* axis. In addition, the relative rotations of the [$Al2O_4$] and [SiO_4] tetrahedra within the *a*-*b* plane also contribute to the compressional anisotropy of the structure (see below).

Comparison of structural changes with pressure and temperature

In a number of silicate minerals, structural changes resulting from increasing pressure are opposite to those caused by increasing temperature (Hazen and Finger 1982). For alumiosilicates, high-pressure structure studies of Ralph et al. (1984) on andalusite and Yang et al. (1997a) on kyanite demonstrated that this inverse relationship holds only qualitatively because of the different response of two structures to temperature and pressure. Compared to andalusite and kyanite, sillimanite shows even more pronounced deviation of the structural changes from the inverse relationship. In andalusite and kyanite, the most and least thermally expandable directions correspond approximately to the most and least compressible directions, but in sillimanite the direction of the least compressibility is along ***c***, whereas the direction of the least thermal expansivity is along ***a*** (Skinner et al. 1961; Winter and Ghose, 1979) (Fig. 5). These observations can be explained in terms of different behavior of the [$Al2O_4$] and [SiO_4] tetrahedra at high temperature and pressure. Winter and Ghose (1979) noted that the relatively rigid [$Al2O_4$] and [SiO_4] tetrahedra both rotate in the same direction (clockwise) with increasing temperature. However, the two different tetrahedra rotate in the opposite directions with increased pressure, with the [$Al2O_4$] tetrahedron rotating anticlockwise and the [SiO_4] tetrahedron clockwise, as shown by the changes in their out-of-plane tilting angles. According to Winter and Ghose (1979), a clockwise rotation of the tetrahedra facilitates the expan-

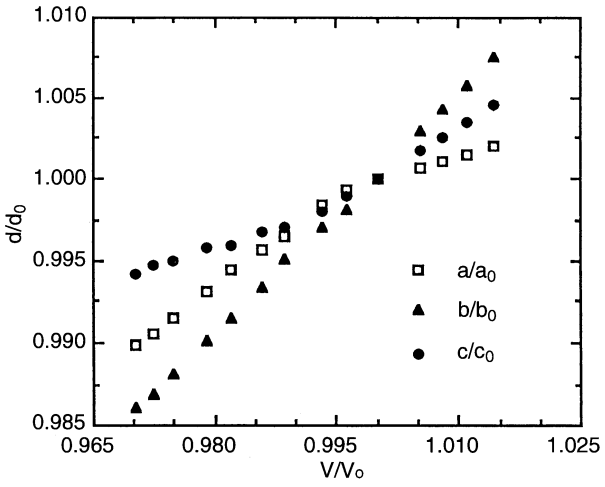

Fig. 5 Ratios of unit-cell dimensions (d/d_0) vs. V/V_0 for sillimanite. High-temperature data are taken from Winter and Ghose (1979)

sion along ***b*** and works against the expansion along ***a***. As a result, the linear thermal expansion coefficient of the *a* dimension at 800°C (α_a=0.19×10^{-5}/°C) is only about half that of the *c* dimension (α_c=0.44×10^{-5}/°C). In fact, the α_a value in sillimanite is the smallest linear thermal expansion coefficient in all three Al_2SiO_5 polymorphs up to 800°C. Consequently, the volume thermal expansion coefficient of sillimanite at 800°C (α_V=1.36×10^{-5}/°C) is smaller than that of kyanite (α_V=2.42×10^{-5}/°C) (Winter and Ghose 1979), in spite of the fact that sillimanite is more compressible than kaynite at high pressure. With increasing pressure, the clockwise rotation of the [SiO_4] tetrahedron becomes a factor contributing to the compression of the *a* dimension, resulting in *a* being more compressible than *c*.

Burnham (1963) noted that the displacement factor of the OC atom, which is only bonded to the Al2 and Si atoms, is nearly twice as great as that of the other oxygen atoms in the sillimanite structure. A similar result has been observed in other structure refinements (Winter and Ghose 1979; Peterson and McMullan 1986), including the present study (Table 2). Burnham (1963) suggested that the large displacement factor of OC could be due to the static positional disorder as compensation for a local charge imbalance on the OC atom and further proposed that a low-temperature structure refinement would help to determine the cause for this. If the OC atom has static positional disorder, its displacement factor should not diminish with decreasing temperature; however, if the large displacement factor actually represents thermal vibration, it will be measurably reduced at low temperature. No low-temperature structure study on sillimanite has been undertaken thus far. Since pressure and temperature may be often considered as opposite variables (Hazen and Finger 1982), our high-pressure data might contain information regarding the abnormally large displacement factor of OC. However, differing from low temperature, high pressure has little influence on atomic displacement factors that primarily represent thermal vibration (Finger and King 1978); instead, it could considerably reduce large atomic displacement factors that result predominately from statically positional disorder, as found in akermanite (Yang et al. 1997b). From room pressure to 5.29 GPa, the magnitude of the OC displacement factor decreases by 16(8)%, the largest decrease of all atomic displacement factors in the sillimanite structure. This observation could favor the suggestion of Burnham (1963). Nevertheless, the amount of the decrease is only two standard deviations up to 5.29 GPa. It is, therefore, difficult for our data to rule out the possibility that the large displacement factor of OC is a real representation of thermal vibration.

Acknowledgements We thank P.J. Dunn of National Museum of Natural History, the Smithsonian Institution for providing us with the sillimanite (NMNH 139740) and andalusite (NMNH R3717) samples. X-ray diffraction work and postdoctoral fellowship to H.Y. at the Geophysical Laboratory are supported by NSF grant EAR-9218845 and by the Carnegie Institution of Washington.

References

Angel RJ (1988) High-pressure structure of anorthite. Am Mineral 73:1114–1119

Becker PJ, Coppens P (1975) Extinction within the limit of validity of the Darwin transfer equations: III. Non-spherical crystals and anisotropy of extinction. Acta Crystallogr A31:417–425

Brace WF, Scholz CH, La Mori PN (1969) Isothermal compressibility of kyanite, andalusite, and sillimanite from synthetic aggregates. J Geophys Res 74:2089–2098

Burnham CW (1963) Refinement of the crystal structure of sillimanite. Z Krystallogr 118:127–148

Burnham CW, Buerger MJ (1961) Refinement of the crystal structure of andalusite. Z Krystallogr 115:269–290

Comodi P, Mellini M, Zanazzi PF (1990) Scapolites: variation of structure with pressure and possible role in the storage of fluids. Eur J Mineral 2:195–202

Comodi P, Mellini M, Ungaretti L, Zanazzi PF (1991) Compressibility and high pressure structure refinement of tremolite, pargasite and glaucophane. Eur J Mineral 3:485–499

Downs RT, Hazen RM, Finger LW (1994) The high-pressure crystal chemistry of low albite and the origin of the pressure dependency of Al-Si ordering. Am Mineral 79:1042–1052

Finger LW, King H (1978) A revised method of operation of the single-crystal diamond cell and refinement of the structure of NaCl at 32 kbar. Am Mineral 63:337–342

Finger LW, Prince E (1972) Neutron diffraction studies: Andalusite and sillimanite. Carnegie Inst Wash Year Book:71:486–500

Finger LW, Prince E (1975) A system of FORTRAN IV computer programs for crystal structure computations. National Bureau of Standards Technology Note 854

Grew ES (1980) Sillimanite and ilmenite from high-grade metamorphic rocks of Antarctica and other areas. J Geology 21:39–68

Grew ES, Rossman GR (1976) Iron in some Antarctic sillimanites. Trans Am Geophys Un 57:337

Hazen RM, Finger LW (1979) Polyhedral tilting: a common type of pure displacive phase transition and its relationship to analcite at high pressure. Phase Transitions 1:1–22

Hazen RM, Finger LW (1982) Comparative Crystal Chemistry. Wiley, New York

Hazen RM, Finger LW (1985) Crystals at high pressure. Sci American 252:110–117

Hemingway BS, Robie RA, Evans HT, Kerrick DM (1991) Heat capacities and entropies of sillimanite, fibrolite, andalusite, kyanite, and quartz and the Al_2SiO_5 phase diagram. Am Mineral 76:1597–1613

Holdaway MJ (1971) Stability of andalusite and the aluminum silicate phase diagram. Am J Sci 271:97–131

Ibers JA, Hamilton WC (1974) International tables for X-ray crystallography. Vol. IV, 366 p. Kynoch, Birmingham, UK

Kerrick DM (1990) The Al_2SiO_5 polymorphs. Min Soc Am Rev Mineral, 22

Kieffer SW (1979) Thermodynamics and lattice vibrations of minerals. 2. Vibrational characteristics of silicates. Rev Geophys Space Phys 17:20–34

King HE, Finger LW (1979) Diffracted beam crystal centering and its application to high-pressure crystallography. J Appl Crystallogr 12:374–378

Lehmann MS, Larsen FK (1974) A method for location of the peaks in step-scan-measured Bragg reflexions. Acta Crystallogr A30:580–584

Mao HK, Xu J, Bell PM (1986) Calibration of the ruby pressure gauge to 800 kbar under quasi-hydrostatic conditions. J Geophys Res 91:4673–4676

Matsui M (1996) Molecular dynamics study of the structures and bulk moduli of crystals in the system CaO-MgO-Al2O3-SiO2. Phys Chem Minerals 23:345–353

Papike JJ, Cameron M (1976) Crystal chemsitry of silicate minerals of geophysical interest. Rev Geophys Space Phys 14:37–80

Peterson RC, McMullan RK (1986) Neutron diffraction studies of sillimanite. Am Mineral 71:742–745

Ralph RL, Finger LW, Hazen RM, Ghose S (1984) Compressibility and crystal structure of andalusite at high pressure. Am Mineral 69:513–519

Ribbe PH (1980) Aluminum silicate polymorphs and mullite. Min Soc Am Rev Mineral:5, 189–214

Robie RA, Hemingway BS (1984) Entropies of kyanite, andalusite, and sillimanite: additional constraints on the pressure and temperature of the Al_2SiO_5 triple point. Am Mineral 69: 298–306

Robinson K, Gibbs GV, Ribbe PH (1971) Quadratic elongation: A quantitative measure of distortion in coordination polyhedra. Science 172:567–570

Skinner BJ, Clark SP, Appleman DE (1961) Molar volumes and thermal expansions of andalusite, kyanite, and sillimanite. Am J Sci 259:651–668

Vaughan MT, Weidner DJ (1978) The relationships of elasticity and crystal structure in andalusite and sillimanite. Phys Chem Minerals 3:133–144

Winter JK, Ghose S (1979) Thermal expansion and high-temperature crystal chemistry of the Al_2SiO_5 polymorphs. Am Mineral 64:573–586

Taylor WH (1928)The structure of sillimanite and mullite. Z Kristallogr 71:205–218

Yang H, Downs RT, Finger LW, Hazen RM, Prewitt CT (1997a) Compressibility and crystal structure of kyanite, Al_2SiO_5, at high pressure. Am Mineral 82:467–474

Yang H, Hazen RM, Downs RT, Finger LW (1997b) Structural change associated with the incommensurate-normal phase transition in akermanite, $Ca_2MgSi_2O_7$, at high pressure. Phys Chem Minerals 24:510–519